Journal of Water Process Engineering 51 (2023) 103466

Contents lists available at ScienceDirect

Journal of Water Process Engineering

journal homepage: www.elsevier.com/locate/jwpe

Efficient removal of antibiotics from water via aqueous portlandite carbonation

G. Montes-Hernandez [a,*], L. Feugueur [a], C. Vernier [a], A.E.S. Van Driessche [a,b], F. Renard [a,c]

[a] ISTerre, Univ. Grenoble Alpes, Grenoble INP, Univ. Savoie Mont Blanc, CNRS, IRD, Univ. Gustave Eiffel, 38000 Grenoble, France
[b] Instituto Andaluz de Ciencias de la Tierra (IACT), CSIC – University of Granada, Armilla, Granada E-18100, Spain
[c] The Njord Centre, Departments of Geosciences and Physics, University of Oslo, Norway

ARTICLE INFO

Keywords:
Antibiotic
Removal
Wastewater
Carbonation
Portlandite
Magnetite
Flow-through curves
Isotherms

ABSTRACT

Current wastewater treatment technologies struggle to remove antibiotics from wastewaters, leading to contamination of surface and groundwater. Therefore, more effective and efficient processes for removing antibiotics from water are needed. The present study reports for the first time that three widely used antibiotics (amoxicillin, ceftriaxone, cefazoline) can be successfully removed from water under ambient conditions by using aqueous carbonation of portlandite. Breakthrough curves acquired from flow-through experiments and their respective removal isotherms were mainly used to determine quantitative equilibrium parameters. In this way, the removal of antibiotics using aqueous portlandite carbonation is very efficient for amoxicillin (9.5 mg/g), followed by cefazoline (4.3 mg/g) and ceftriaxone (2.7 mg/g). In a comparison perspective, nanomagnetite-interfacial Fenton reaction is more effective in removing amoxicillin (76.5 mg/g); however, the process is slower and chemically more complex. However, both investigated methods offer promising results at the laboratory scale and are technically feasible to be implemented in conventional and/or advanced wastewater treatment plants.

1. Introduction

De novo designed organic molecules, including pharmaceuticals, hormones, personal care products, surfactants, drugs, and pesticides, are a serious source of contaminants in water. Among these pollutants are antibiotics, the most frequently prescribed drug of modern human medicine, which are also widely used in the animal farming industry, including cattle, swine, poultry, and fish. The benefits of antibiotics in healthcare of human and animals are undisputed. However, excessive and wrong usage raises the risk of drug resistance in the environment, leading to the most common antibiotics being no longer effective in controlling infectious diseases [1–5]. Antibiotics from different sources (e.g. municipal waste water, hospitals, animal production, and pharmaceutical industries) are ultimately discharged into wastewater treatment plants. However, conventional and advanced treatment plants are not effective in removing antibiotics leading to the release of these compounds in surface and groundwater [6,7]. In the last two decades, various methods to remove and/or degrade antibiotics from water have been investigated in the laboratory and frequently tested in pilot or plant scale, including biodegradation, nanofiltration, advanced oxidation processes, photocatalytic degradation, reverse osmosis, ozonation and adsorption [8–15]. Among these methods, adsorption appears to be a suitable technique to remove various antibiotics from contaminated water and industrial effluents because of its high efficiency, simple design, easy operation and its ability to remove a wide range of contaminant concentrations. High specific surface areas (>500 m^2/g) and microporous materials (e.g. metal–organic frameworks – MOFs) are frequently required; but in general, diversified natural or synthetic materials (including green and low-cost materials) have been tested to remove antibiotics [16–18]. Mineral precipitation has also been suggested as an economic and robust method to remove ionic and organic pollutants from water; for example, calcite precipitation can remove several heavy metals and metalloids from water, but rarely organic pollutants [19,20].

In the present study we show that calcite precipitation via aqueous portlandite carbonation ($Ca(OH)_2 + CO_2 \Rightarrow CaCO_3 + H_2O$) in a flow-through reactor at ambient conditions is a simple method to effectively remove three types of antibiotics (amoxicillin, ceftriaxone and cefazolin). This carbonation method has been investigated in order to produce nanosized calcite under mild and hydrothermal conditions or in

* Corresponding author.
E-mail address: german.montes-hernandez@univ-grenoble-alpes.fr (G. Montes-Hernandez).

https://doi.org/10.1016/j.jwpe.2022.103466
Received 13 October 2022; Received in revised form 22 December 2022; Accepted 22 December 2022

order to sequester ionic pollutants from water [19,20]. In this way, based on breakthrough curves and respective sequestration isotherms we establish the efficiency of this approach. In addition, we show, using the same flow-through setup, that a Fenton-type oxidation reaction using magnetite nanoparticles is also an efficient process to remove amoxicillin. However, this oxidation reaction requires low pH (pH < 3), a significant amount of oxygenated water and a ferrous source (Fe(II) as enhancing reaction agents.

2. Materials and methods

2.1. Chemicals

Four antibiotics (amoxicillin ($C_{16}H_{19}N_3O_5S$), erythromycin ($C_{37}H_{67}NO_{13}$), ceftriaxone ($C_{18}H_{18}N_8O_7S_3$), cefazolin ($C_{14}H_{14}N_8O_4S_3$)) and soluble salts (calcium chloride dihydrate ($CaCl_2.2H_2O$), ferrous chloride dihydrate ($FeCl_2.2H_2O$), ferric chloride heptahydrate ($FeCl_3.6H_2O$) and sodium hydroxide (NaOH)) with high purity (>99 %) were obtained from Sigma-Aldrich. All reactants were used as received. Carbon dioxide (CO_2) was obtained from Linde Gas S.A. with 99.995 % of chemical purity. This gas was used as received and directly bubbled into the antibiotic inlet solutions. Deionized water (18.2 MΩ of resistivity) used in the synthesis of minerals, drinking water of the city of Grenoble (its ionic composition and/or chemistry was already reported in a previous study [21]) used in flow-through and batch experiments and oxygenated water (H_2O_2) at 30 % (provided by Sigma-Aldrich) and chloride acid (HCl) at 10 % (provided by Sigma-Aldrich) used in the Fenton's reaction.

2.2. Minerals

Portlandite platy nanoparticles ($Ca(OH)_2$ with hexagonal shape and with 16 m^2/g of specific surface area) were synthesized using a coprecipitation method in alkaline medium ($Ca^{2+} + 2OH^- \Rightarrow Ca(OH)_2$) by rapid mixing of 100 mL of calcium chloride solution (1 M) with 210 mL of sodium hydroxide (1 M) at room temperature. The resulting suspension was stirred for 15 min and then the precipitate was recovered by filtration and washed with deionized water. Finally, the portlandite was dried in a CO_2-free atmosphere at 60 °C for 24 h.

Magnetite spherical nanoparticles (Fe_3O_4 with size<20 nm, with 28 m^2/g of specific surface area) were synthesized using a coprecipitation method by adding 200 mL of a mixed-valent iron solution (1 M, ($Fe^{2+} + Fe^{3+}$), pH ~ 1) with a controlled flow rate (2.3 mL/min) to 200 mL of NaOH solution (4 M, pH = 14) at room temperature under constant stirring. The reaction mechanism and kinetics for this coprecipitation reaction have been previously investigated by time-resolved Raman spectroscopy [22].

Calcite nanoparticles ($CaCO_3$ with size<100 nm, with 9 m^2/g of specific surface area) was synthesized by aqueous carbonation of portlandite with compressed CO_2 (55 bar) at room temperature, following the overall reaction: $Ca(OH)_2 + CO_2 \Rightarrow CaCO_3 + H_2O$. The mineral composition, kinetics, and reaction mechanisms were determined by time-resolved Raman spectroscopy measurement [23].

2.3. Flow-through reactor experiments

2.3.1. Aqueous carbonation of portlandite

Two flow-through reactors with 50 mL internal volume were first filled with Grenoble drinking water, ionic composition reported in Hajji et al. [21]. One reactor also contained 1 g of synthetic portlandite (reactive tracer reactor). The other reactor without mineral-reactant was used as a reference (inert tracer reactor). An antibiotic-rich solution (2 L with 100–120 mg/L of a given antibiotic) was constantly bubbled with CO_2 in a beaker. Then, this CO_2-saturated antibiotic solution was simultaneously percolated through both reactors at a constant rate of 12.2 mL/min for 80 min at room temperature (20 °C). The mineral-solution suspension in the flow-through reactor was continuously stirred using a magnetic Teflon bar. The outflow solutions from the inert and reactive tracer reactors were filtered in situ through 0.2 μm pore size Teflon membranes located on the top of the reactors. The antibiotic concentration in filtered solutions at various times of the experiment (0.5, 2, 5, 10, 15, 20, 80 min) were determined with Ultraviolet-Visible (UV–Vis) spectroscopy (Agilent Cary 60). We used calibration lines for amoxicillin ($C_{amoxicillin} = A/0.0216$) at 228 nm (where C is concentration and A is the absorbance), ceftriaxone ($C_{ceftriaxone} = A/0.0444$) at 237 nm and cefazolin ($C_{cefazolin} = A/0.0236$) at 273 nm. These measurements were used to determine experimental breakthrough curves for the solutions of the inert and reactive tracer reactors, as previously described for As and Cr sequestration by using nanostructured synthetic minerals [21]. All experiments were repeated at least two times in order to confirm their reproducibility.

2.3.2. Fenton reaction

The same experimental setup as described above was used to investigate the oxidation process of amoxicillin. Here, 1 g of magnetite nanoparticles was placed in the reactive tracer reactor and provided a ferrous iron source for the Fenton reaction at the magnetite-solution interfaces. The inlet solution containing amoxicillin (2 L with 120 mg/L) was modified to activate the Fenton reaction by adding 1.2 mL of 30 % oxygenated water (H_2O_2) and adjusting the pH to 2.6 by adding HCl. This solution was simultaneously flown through both (inert and reactive) reactors at a rate of 2.3 mL/min during 7 h. Solution samples were retrieved at different time intervals (outlet solutions from inert and reactive tracer reactors) and analyzed by UV–Vis spectroscopy in order to measure the evolution of the amoxicillin concentration and determine the respective breakthrough curves.

2.3.3. Calculation of removal isotherms

The experimental breakthrough curves obtained from the inert and reactive tracer reactors were used to determine the removal isotherm for a given antibiotic. The corresponding removed fraction between $C = 0$ and C_i was calculated by integrating the surface area between the breakthrough curves of the inert and reactive tracers inside of a given interval of time. Each of these calculations provided one point (C_i, q_i) of the isotherm; assuming an equilibrium concentration in each point as explained in Limousin et al. [24]. The relationship to determine the removed amount ($q_i = q_e$) for a given equilibrium concentration ($C_i = C_e$) from breakthrough curves writes as follows:

$$q_i = \frac{\text{Flow rate}}{\text{Solid mass}} A_i = \frac{\text{Flow rate}}{\text{Solid mass}} \left(\int_{t=0}^{t=t_i} C_{\text{inert tracer}}\, dt - \int_{t=0}^{t=t_i} C_{\text{reactive tracer}} dt \right) \quad (1)$$

The main advantage of this method is that only one percolation experiment for inert and reactive tracer reactors is required to determine one isotherm for a given pollutant. Finally, all removal isotherms obtained from breakthrough curves were fitted using Hill's model ($q_e = \frac{q_{e(max)} C_e^b}{K^b + C_e^b}$ with $q_{e(max)}$, K and b fitting parameters) than can describe sigmoidal complex behaviors, and, in several cases, is equivalent to the Langmuir adsorption model.

2.4. Batch reactor experiments

Aqueous carbonation of portlandite in the presence of antibiotic was also monitored in real time with Raman spectroscopy in order to identify the effect of antibiotics on the nucleation process of calcite. Here, 2 g of synthetic portlandite was dispersed in 200 mL of an antibiotic solution (100 mg/L) placed inside of a hydrothermal reactor equipped with an in-situ Raman probe (RAMAN RXN1, Kaiser Optical Systems). Then, 5–10 bar of CO_2 was injected in the reactor and the system was monitored during 20–60 min at a rate of one acquisition every 0.25 or 1 min. This custom-build experimental setup has been used to investigate the

nucleation, growth and transformation of several mineral phases [23,25–27].

For the Fenton reaction, two additional experiments were performed using 2 L beakers. Here, 1 L of amoxicillin solution (130 mg/L, 0.6 mL of oxygenated water at pH = 2.55) was stirred in the presence of 1 g of magnetite nanoparticles. Several fluid samples were withdrawn at different time intervals and the amoxicillin concentration was determined with UV–Vis spectroscopy.

2.5. Ex situ characterization of solids

Selected recovered solid samples were dried under air atmosphere at 60 °C for 48 h and stored in plastic flasks for subsequent characterization by Field-Emission Scanning Electron Microscopy (FESEM) and powder X-ray diffraction (PXRD).

XRD patterns were acquired using a Siemens D5000 diffractometer in Bragg-Brentano geometry, equipped with a theta-theta goniometer with a rotating sample holder. Diffraction patterns were then collected using Cu kα$_1$ ($\lambda_{k\alpha1}$ = 1.5406 Å) and Cu kα$_2$ ($\lambda_{k\alpha2}$ = 1.5444 Å) radiations in the range 2θ = 10–70°, with a step size of 0.04° and a counting time of 6 s per step. Coherent average size of some samples was systematically refined by the quantitative Rietveld method on XRD patterns using the BGMN software and its associated database [28].

Concerning the high-resolution microscopy imaging, the solid products were dispersed by ultrasonic treatment in high purity water for 5 min. One droplet of the suspension was then deposited directly on an aluminum support and observed without metal coating because calcite and magnetite nanoparticles have enough conductivity. The powder was imaged using a Zeiss Ultra 55 FESEM with a maximum spatial resolution of ca. 1 nm at 15 kV.

3. Results and discussion

3.1. Removal of antibiotics by portlandite aqueous carbonation

During a representative carbonation reaction of portlandite (Ca(OH)$_2$) in a CO_2-saturated solution, first the portlandite particles dissolve and release Ca^{2+}. Immediately, amorphous calcium carbonate (ACC) particles precipitate, and transform into calcite ($CaCO_3$) within a few seconds to minutes, as demonstrated by previous time-resolved Raman spectroscopy measurements [23]. In this way, the calcite growth process can incorporate, adsorb and/or enhance precipitation of ionic elements (Se, As, Cr, Fe, Mn, Sb, P and N) from polluted solutions, [19,20,29–35] and also remove organic pollutants such as antibiotics as demonstrated in the present study.

Herein, we assessed the efficiency of the antibiotic removal via aqueous portlandite carbonation by comparing breakthrough curves obtained simultaneously from the inert and reactive tracer reactors. In our experimental setup, if the pollutant does not have any physiochemical affinity and/or reactivity with the dispersed solid particles, the breakthrough curves for inert and reactive tracers should overlap. However, if some interaction with the dispersed particles occurs, the breakthrough curve for the reactive tracer may display a significant retarding effect with respect to the breakthrough curve of the inert tracer. In such case, a removal isotherm can be calculated by using Eq. (1). Figs. 1 and 2 show breakthrough curves and removal isotherms for amoxicillin in the presence of different starting amounts of portlandite. These curves reveal that a significant amount of amoxicillin is removed during aqueous carbonation of portlandite. This process is directly related to initial available portlandite (1 or 2 g). The retarding of reactive tracer curve is also proportional to the initial dose (see breakthrough curves in Figs. 1 and 2). These results thus show that amoxicillin is sequestered during the carbonation process of portlandite, i.e. when calcite is forming. A control experiment was performed where high purity calcite was used as potential sequestration agent. In this case, breakthrough curves for inert and reactive tracers overlap (see Fig. SI-1), indicating negligible amoxicillin sorption/sequestration onto already formed calcite particles. This result thus further confirms that amoxicillin is being retained from solution during the initial stages of calcite formation.

The removal isotherms for amoxicillin, i.e. the removed amount as a function of equilibrium concentration, are equivalent when 1 or 2 g of portlandite are used (Figs. 1 and 2 on the right). This result is consistent because the removed amount of amoxicillin was normalized with portlandite mass and an equilibrium concentration in the percolating solution was assumed in these flow-through experiments. Specifically, the fitted parameters from Hill's model show that the equilibrium constant K (equilibrium concentration, which represents also the half-removed amount of pollutants), the maximum removed amount, $q_{e(max)}$, and Hill's coefficient, b, are equivalent for both initial quantities of portlandite. K and $q_{e(max)}$ are two fundamental parameters to calculate the liquid-solid distribution coefficients ($K_D = q_{e(max)}/K$, given in [L/g]). K_D is widely used to simulate the mass transfer at the solid-fluid interfaces in porous media [19]. Table 1 provides these parameters for all fitted isotherms.

The removal of two other antibiotics (ceftriaxone and cefazolin) was

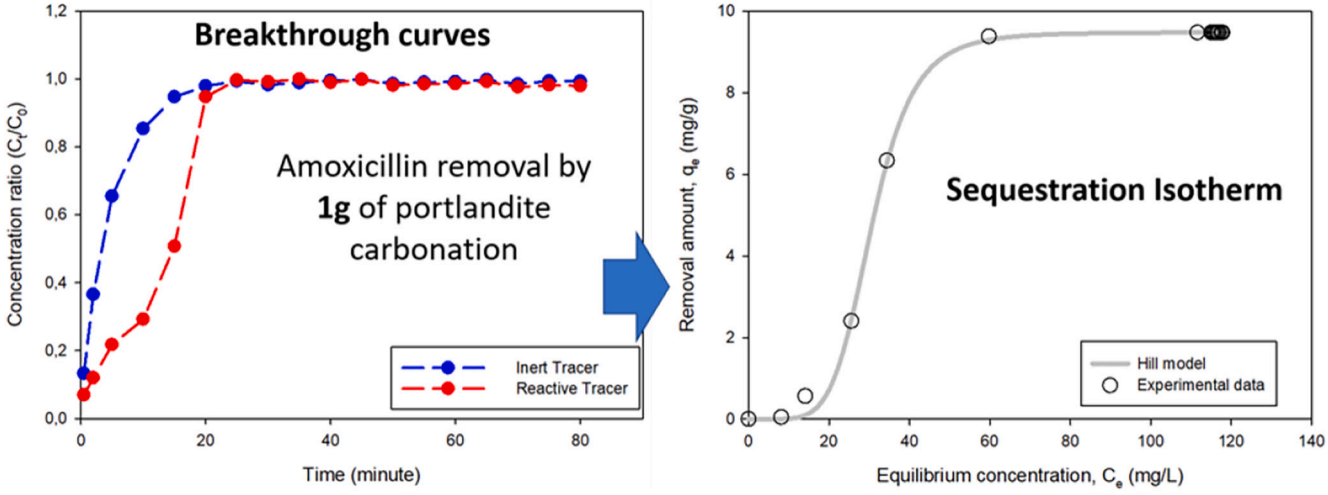

Fig. 1. Removal of amoxicillin from CO_2-saturated solutions via portlandite carbonation. Left: Experimental breakthrough curves for inert tracer (reactor without portlandite) and reactive tracer (reactor with portlandite (1 g)) (standard deviation<5 % after equilibration of curves). Right: Amoxicillin removal isotherm from breakthrough curves determined by Eq. (1) and data fitted by Hill model (error of fitted parameters provided in Table 1).

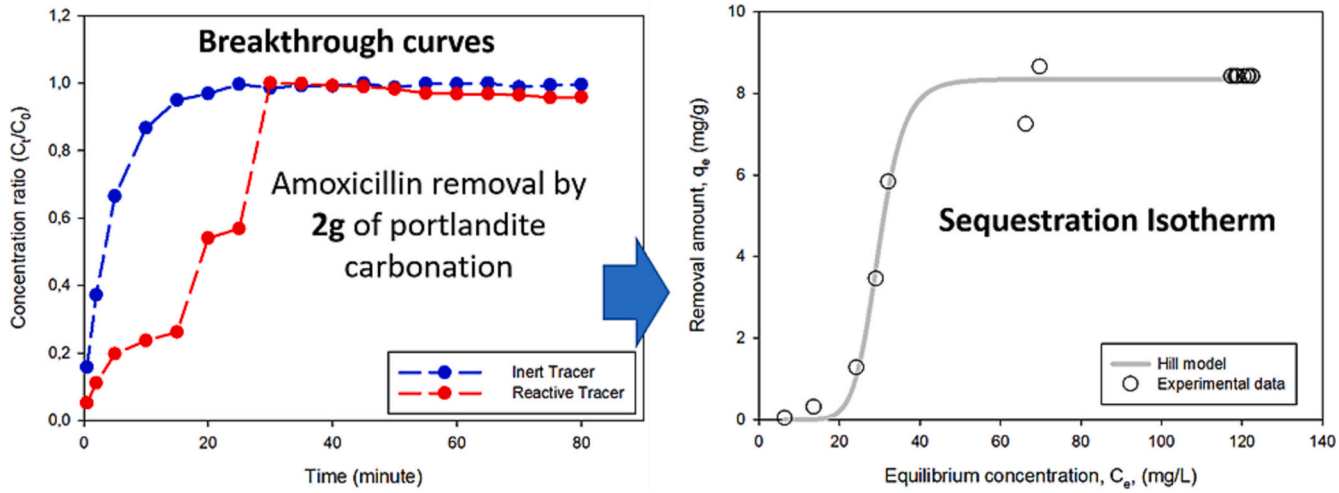

Fig. 2. Removal of amoxicillin from CO_2-saturated solutions via portlandite carbonation. Left: Experimental breakthrough curves for inert tracer (reactor without portlandite) and reactive tracer (reactor with portlandite (2 g)) (standard deviation<7 % after equilibration of curves). Right: Amoxicillin removal isotherm from breakthrough curves determined by Eq. (1) and data fitted by Hill model (error of fitted parameters provided in Table 1).

Table 1
Summary of equilibrium parameters from Hill's model used to fit the data of the removal of antibiotics from water by portlandite aqueous carbonation and by nanomagnetite-interfacial Fenton reaction. Experimental isotherms were determined from breakthrough curves (Eq. (1)).

Antibiotic	Mineral	Parameters used to fit Hill's model			$K_D = q_{e(max)}/K$ L/g	Process
		K mg/L	$q_{e(max)}$ mg/g	b		
Amoxicillin	Portlandite (1 g)	30.62 ± 0.22	9.48 ± 0.03	5.84 ± 0.27	0.30	Aqueous carbonation
Amoxicillin	Portlandite (2 g)	29.74 ± 0.36	8.35 ± 0.09	9.32 ± 1.35	0.28	Aqueous carbonation
Cefazolin	Portlandite (1 g)	56.10 ± 0.73	4.27 ± 0.04	10.11 ± 1.24	0.08	Aqueous carbonation
Ceftriaxone	Portlandite (1 g)	66.59 ± 0.49	2.69 ± 0.02	16.43 ± 1.81	0.04	Aqueous carbonation
Amoxicillin	Magnetite nanoparticles (1 g)	130.75 ± 22.02	76.52 ± *	9.30 ± 1.48	0.58	Fenton reaction

K: equilibrium concentration producing half-removed amount, $q_{e(max)}$: maximum removed amount, b: Hill's coefficient, K_D: liquid-solid distribution coefficient, *:very high error.

also assessed. Figs. 3 and 4 show the breakthrough curves and the removal isotherms for cefazolin and ceftriaxone, respectively. These data show that both antibiotics are also efficiently removed from solution by aqueous carbonation of portlandite. The removed amount versus equilibrium concentration follows a similar trend for both antibiotics and the removal isotherms were again fitted using Hill's model (Table 1). In summary, significant amounts of amoxicillin, ceftriaxone, and cefazoline can be removed by aqueous carbonation of portlandite. The plateaus in the isotherm curves of Figs. 1, 2, 3, and 4 (on the right) show that the method is most efficient for amoxicillin (9.5 mg/g), followed by cefazoline (4.3 mg/g) and ceftriaxone (2.7 mg/g). Erythromycin was also assessed, unfortunately, this antibiotic has low absorbance in UV vis spectroscopy at the investigated concentration. For this reason, only qualitative results are commented in the following paragraphs.

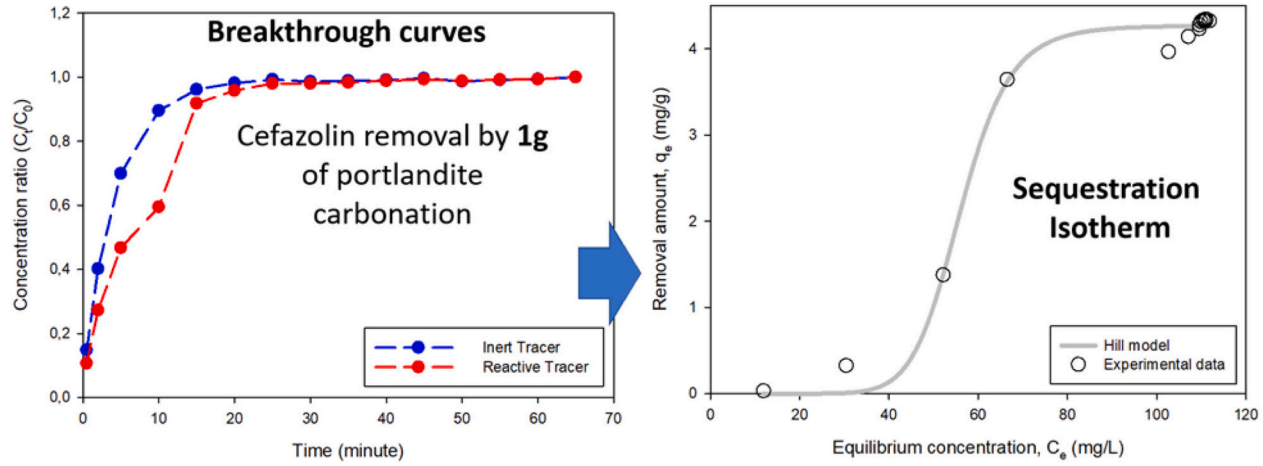

Fig. 3. Left: Experimental breakthrough curves for inert tracer (reactor without portlandite) and reactive tracer (reactor with portlandite (1 g)) concerning cefazolin removal by aqueous carbonation of portlandite ((standard deviation<5 % after equilibration of curves). Right: Cefazolin removal isotherm from breakthrough curves determined by Eq. (1) and data fitted by Hill model (error of fitted parameters provided in Table 1).

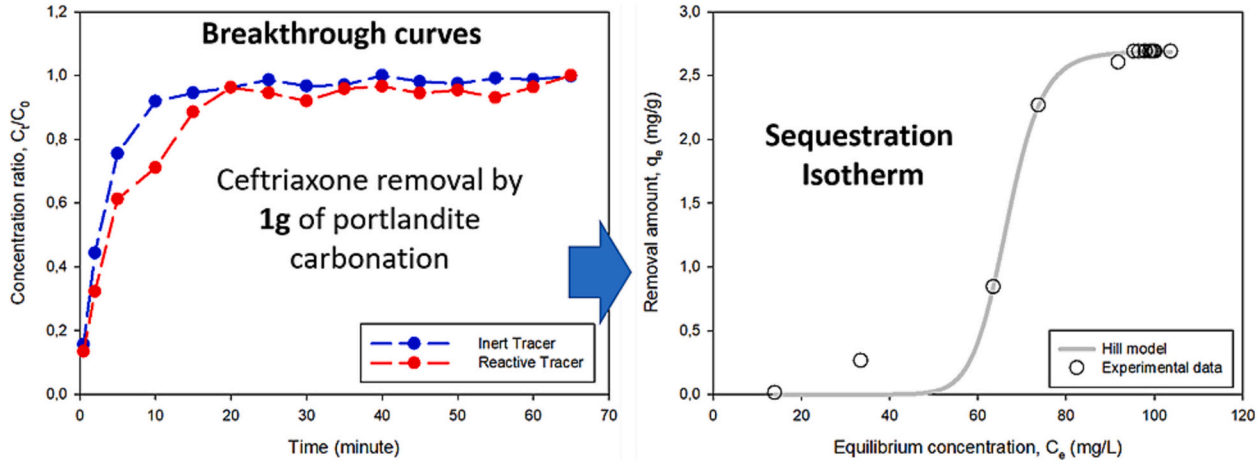

Fig. 4. Left: Experimental breakthrough curves for inert tracer (reactor without portlandite) and reactive tracer (reactor with portlandite (1 g)) concerning ceftriaxone removal by aqueous carbonation of portlandite (standard deviation<7 % after equilibration of curves). Right: Ceftriaxone removal isotherm from breakthrough curves determined by Eq. (1) and data fitted by Hill model (error of fitted parameters provided in Table 1).

Noteworthy, the UV–Vis spectroscopy data reveal that the absorbance peak for amoxicillin, cefazoline and ceftriaxone shifts to a higher wavelength in portlandite alkaline media. For example, amoxicillin absorbance shifts from 228 nm (typical in water) to 247 nm in a saturated portlandite solution (Fig. SI-2). This is probably due to a strong complexation of amoxicillin with Ca^{2+} in an alkaline solution because such peak shifts back to typical absorbance wavelength in water (i.e. 228 nm) when all portlandite was consumed in the system, i.e. when calcite precipitation had finished during a percolation experiment. The observed shifts also agree with a complexation study of amoxicillin in Ca^{2+} systems [36]. The UV–Vis time-resolved spectra during amoxicillin removal by portlandite aqueous carbonation (Fig. 5) may be explained by a selective Ca complexation of this antibiotic under alkaline conditions, a process which could also contribute to antibiotic removal.

To gain insight on the influence of antibiotic on the nucleation of calcite from aqueous carbonation of portlandite additional batch experiments were performed in real time using Raman spectroscopy. Results show that the presence of antibiotics does not change significantly the calcite nucleation mechanism. Amorphous calcium carbonate peaking at 1080 cm^{-1} was detected as the only transient phase and its lifetime varied slightly with the different antibiotics in the range three to 5 min under our experimental conditions (Fig. 6).

FESEM images acquired on the recovered solid phase showed oriented aggregates of calcite crystals (resembling mesocrystals) for all antibiotics, except erythromycin where well-dispersed nanoparticles of calcite were obtained (see Fig. SI-3). Average calcite particle sizes observed in FESEM images agree with the average particle size extracted from powder XRD patterns. In particular, the average particle size for calcite varies when a given antibiotic is used, as revealed by the full wide half maximum (FWHM) parameter. The position of the main reflection (104) varies also slightly, which is probably due to a minor incorporation of the antibiotic into the calcite crystal lattice (see Fig. SI-4).

Our spectroscopic and textural data suggest that complexed antibiotic was mainly removed during the formation and transformation of amorphous calcium carbonate (ACC) into calcite. We interpret that the organic material adhered onto calcite nanoparticles, inducing the formation of mesocrystals, a process that was previously observed during calcite formation via aqueous carbonation of portlandite in presence of common domestic drinks [37].

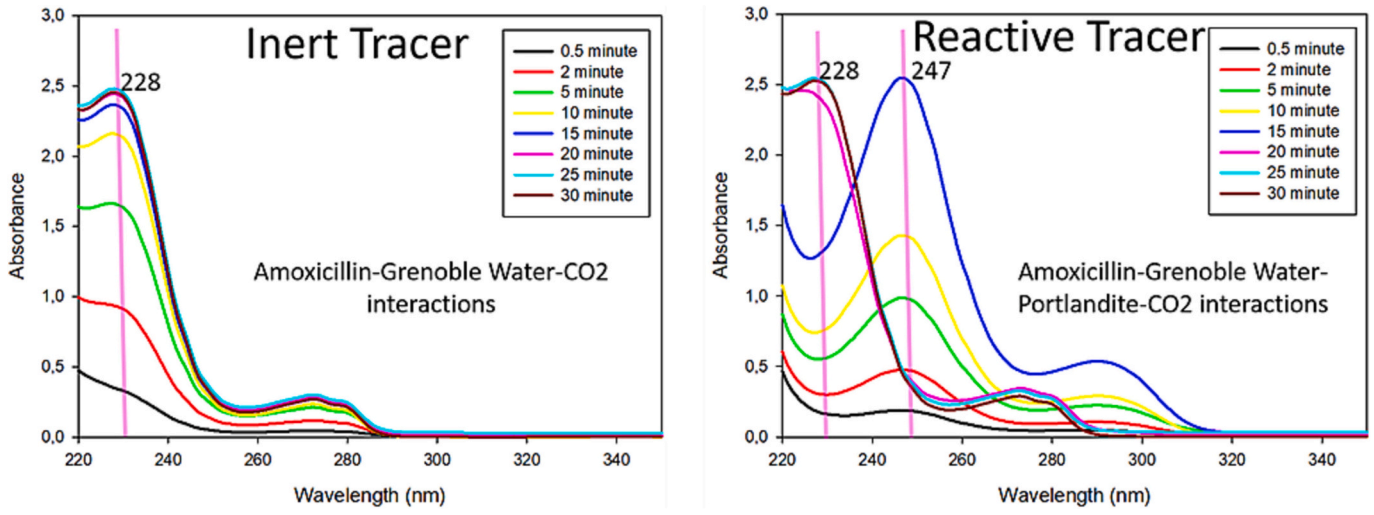

Fig. 5. (Left) Time-lapse UV–Vis spectra for amoxicillin showing data from the inert tracer reactor in the percolation experiment. (Right) Time-lapse UV vis spectra for amoxicillin showing data from the reactive tracer reactor in the percolation experiment. Results indicate that amoxicillin is strongly complexed with calcium during carbonation process of portlandite (see reactive tracer reactor at right) because amoxicillin UV–Vis absorbance backs to typical absorbance when portlandite was completely consumed in the system.

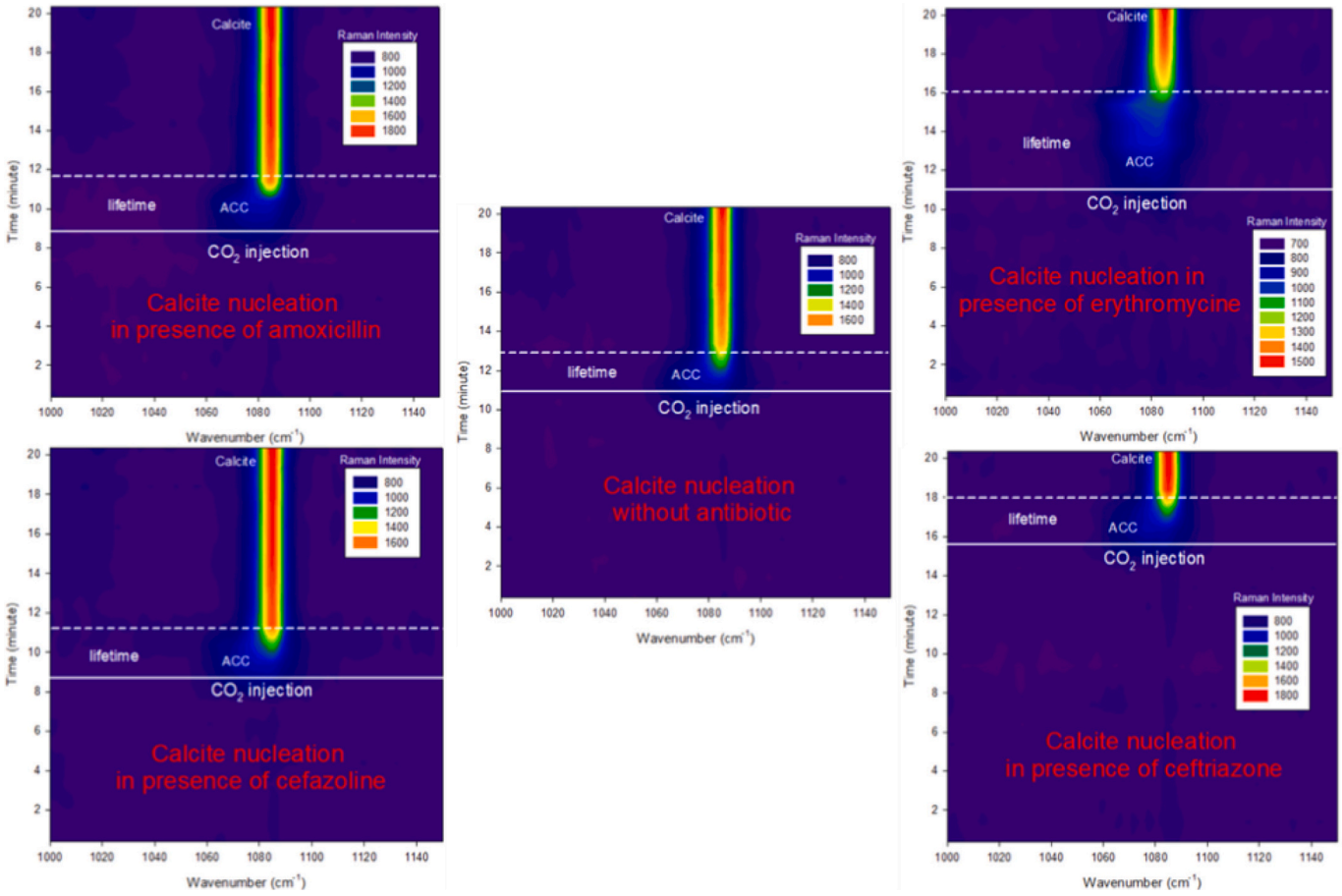

Fig. 6. Time-lapse Raman spectra for calcite nucleation in presence of four different antibiotics, and reference without antibiotic. In all cases, amorphous calcium carbonate (ACC, blue halo on the figures) formed prior to calcite nucleation and was detected after the first minute of CO_2 injection. Its lifetime was similar and close to 3 min for all experiments, except in the presence of erythromycin where it was 5 min. (For interpretation of the references to colour in this figure legend, the reader is referred to the web version of this article.)

3.2. *Removal of amoxicillin by Fenton reaction*

Advanced oxidation of organic pollutants via the so-called Fenton process has been investigated and implemented in modern wastewater plant treatment [38]. For this reason, we investigate here a modified Fenton reaction using nanosized magnetite as ferrous source for amoxicillin removal, in order to compare it with the aqueous carbonation of portlandite method. A typical Fenton oxidation process involves complex redox and decomposition reactions between several reactants (ferrous iron, oxygenated water and antibiotic) at low pH in the range 2.5–3.5. In our experiments, we varied the concentration of oxygenated water, magnetite particle size and pH adjustment. The antibiotic

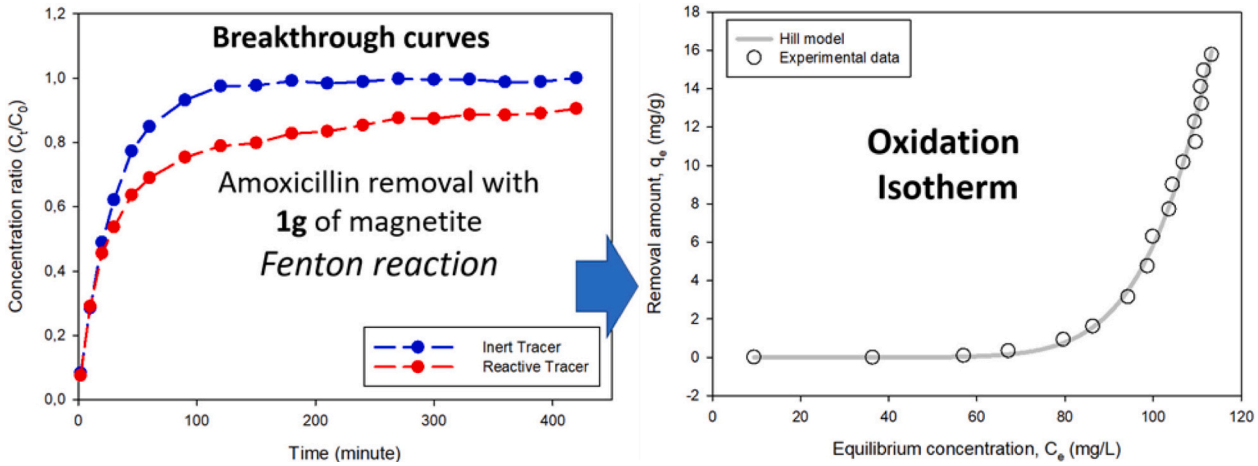

Fig. 7. Left: Experimental breakthrough curves for inert tracer (reactor without magnetite) and reactive tracer (reactor with magnetite (1 g)) during the removal of amoxicillin by aqueous magnetite-interfacial Fenton reaction (standard deviation<5 % after equilibration of inert tracer curve). Right: Amoxicillin removal isotherm from breakthrough curves determined by Eq. (1) and data fitted with Hill's model (error of fitted parameters provided in Table 1).

removal amount was exclusively obtained when the pH was pre-adjusted to 2.6 and when 260 mg/L of oxygenated water and magnetite nanoparticles were used. In this case, the amoxicillin was partially oxidized by Fenton reaction, as revealed by the breakthrough curves for inert and reactive tracers (Fig. 7). Herein, the ferrous iron was provided from surface magnetite dissolution enhanced at low pH in the presence of oxygenated water. Then the oxidation of amoxicillin took place at the surface of the magnetite nanoparticles, including two main reactions taking place at the nanoparticle-solution interface:

$$Fe^{2+} + H_2O_2 \Rightarrow Fe^{3+} + \bullet OH + OH^- \quad (2)$$

$$\text{Antibiotic} + \bullet OH \Rightarrow CO_2 + H_2O + \text{inorganic} - \text{matter} \quad (3)$$

The oxidation and/or degradation process of antibiotics can imply various intermediate steps, as determined for amoxicillin in aquatic environment [39]. In our case, a simpler approach was used by measuring the residual amoxicillin in water during flow-through experiments at different time intervals using UV–Vis spectroscopy. The breakthrough curve for the reactive tracer shown in Fig. 7 reveals a significant retarding with respect to the inert tracer after 7 h of percolation and the reaction is still active because the concentration in the outlet solution has not reached the concentration of the inlet solution. This indicates that the oxidation of amoxicillin is a relatively slow process.

Importantly, the removal isotherm shown in Fig. 7 (on the right) did not reach the maximum amount of removed amoxicillin calculated by Hill's model. This model estimates a maximum removal amount of about 76 mg/g (see Table 1 and projection curve on Fig. SI-6). In order to validate this calculation, we performed several batch reactor experiments (volume 1 L). The obtained data showed that 33 mg of amoxicillin per g of magnetite nanoparticles were removed after 7-24 h (Fig. SI-7). This result agrees well with the flow-through experiments and both experimental configurations indicate that the Fenton reaction was probably passivated by iron oxidation at the magnetite-solution interfaces, but such reactions remained active during several hours in flow-through and batch reactors as demonstrated in the present study. In practice, as expected the interfacial-magnetite Fenton reaction is also an efficient method to remove amoxicillin from water. But, this reaction is not active when the pH is not adjusted to 2.6; here, the amoxicillin oxidation is not active and/or negligible as revealed by an overlapping of breakthrough curves for inert and reactive tracers (Fig. SI-5). A similar inactivation of the Fenton reaction was observed at lower concentrations of oxygenated water and when microparticles of magnetite were used instead of nanoparticles.

4. Conclusion

Amoxicillin can be successfully removed from water using a flow-through setup implementing aqueous carbonation of portlandite or an interfacial-magnetite Fenton reaction. Both methods can efficiently remove these antibiotics from water as demonstrated with breakthrough curves and their respective removal isotherms. The interfacial-magnetite Fenton reaction offers a better removal capacity for amoxicillin with respect to aqueous carbonation of portlandite. Importantly, the solid-liquid separation could be facilitated because the reacting magnetite particles preserve their magnetic potential, and this Fenton reaction can be used to remove organic pollutants from water at an industrial scale. We also assessed the removal capacity of the carbonation method for two other antibiotics, ceftriaxone and cefazoline. In overall, aqueous carbonation of portlandite offers a more promising and easier operating method to remove antibiotics from water because it can be implemented without significant modification of existing water treatment plants, for example, by using coagulation units that are already present in these plants. In our method, the treated water is neutralized with CO_2 during aqueous carbonation of portlandite and the pH at the outlet flow is close to 7. This water could be directly discharged into nature, reused, or undergo additional treatment. In addition, this method can also be used to efficiently remove ionic pollutants such as heavy metals and metalloids (e.g. As, Se and Fe). Moreover, the generated solid product, about 1.35 kg of high purity calcite per m^3 of treated water, can be re-used in a variety of industrial applications such as additive and mineral filler (e.g. plastics, paper, paintings, etc.).

Declaration of competing interest

The authors declare that they have no known competing financial interests or personal relationships that could have appeared to influence the work reported in this paper.

Data availability

No data was used for the research described in the article.

Acknowledgements

The authors acknowledge funding from the French National Centre for Scientific Research (CNRS) and the Université Grenoble Alpes (UGA). We thank Nathaniel Findling for technical assistance with XRD data. The study received funding from ADEME (The French Agency for Ecological Transition) through the project FUNMIN.

Appendix A. Supplementary data

Supplementary data to this article can be found online at https://doi.org/10.1016/j.jwpe.2022.103466.

References

[1] I.T. Carvalho, L. Santos, Antibiotics in the aquatic environments: a review of the european scenario, Environ. Int. 94 (2016) 736–757.
[2] M. Sagaseta de Ilurdoz, J.J. Sadhwani, V. Reboso, Antibiotic removal processes from water & wastewater for the protection of the aquatic environment - a review, J. Water Proc. Eng. 45 (2022), 102474.
[3] M.F. Li, et al., Graphene and graphene-based nanocomposites used for antibiotics removal in water treatment: a review, Chemosphere 226 (2019) 360–380.
[4] S. Zhang, W. Lin, X. Yu, Effects of full-scale advanced water treatment on antibiotic resistance genes in the Yangtze Delta area in China, FEMS Microbiol. Ecol. 92/5 (2016), fiw065.
[5] A.S. Oberoi, et al., Insights into the fate and removal of antibiotics in engineered biological treatment systems: a critical review, Environ. Sci. Technol. 53 (2019) 7234–7264.
[6] A.J. Watkinsona, E.J. Murbyc, S.D. Costanzo, Removal of antibiotics in conventional and advanced wastewater treatment: implications for environmental discharge and wastewater recycling, Water Res. 41 (2007) 4164–4176.
[7] Z. Song, et al., Occurrence, fate and health risk assessment of 10 common antibiotics in two drinking water plants with different treatment processes, Sci. Total Environ. 674 (2019) 316–326.
[8] J. Yu, et al., Removal of antibiotics from aqueous solutions by a carbon adsorbent derived from protein-waste-doped biomass, ACS Omega 5 (2020) 19187–19193.
[9] Y.Z. Yan, et al., Hierarchical multi-porous carbonaceous beads prepared with nano-CaCO3 in-situ encapsulated hydrogels for efficient batch and column removal of antibiotics from water, Microporous Mesoporous Mater. 293 (2020), 109830.
[10] S.R. Zhu, et al., Covalent triazine framework modified BiOBr nanoflake with enhanced photocatalytic activity for antibiotic removal, Cryst. Growth Des. 18 (2018) 883–891.
[11] S.E. Estrada-Flórez, E.A. Serna-Galvis, R.A. Torres-Palma, Photocatalytic vs. Sonochemical removal of antibiotics in water: structure degradability relationship, mineralization, antimicrobial activity, and matrix effects, J. Environ Chem. Eng. 8 (2020), 104359.
[12] Y. Liu, et al., Preparation of magnetic hyper-cross-linked polymers for the efficient removal of antibiotics from water, ACS Sustain. Chem. Eng. 6 (2018) 210–222.
[13] F. Yu, Y. Li, S. Han, J. Ma, Adsorptive removal of antibiotics from aqueous solution using carbon materials, Chemosphere 153 (2016) 365–385.
[14] S. Jia, et al., Removal of antibiotics from water in the coexistence of suspended particles and natural organic matters using amino-acid-modified-chitosan flocculants: a combined experimental and theoretical study, J. Hazard. Mater. 317 (2016) 593–601.
[15] B.L. Phoona, et al., Conventional and emerging technologies for removal of antibiotics from wastewater, J. Hazard. Mater. 400 (2020), 122961.
[16] H.J. Cho, et al., Impact of Zr6 node in a metal−organic framework for adsorptive removal of antibiotics from water, Inorg. Chem. 60 (2021) 16966–16976.

[17] J. Imanipoor, et al., Adsorption and desorption of amoxicillin antibiotic from water matrices using an effective and recyclable MIL-53(Al) metal−organic framework adsorbent, J. Chem. Eng. Data 66 (2021) 389–403.
[18] R. Rostamian, H. Behnejad, A unified platform for experimental and quantum mechanical study of antibiotic removal from water, J. Water Proc. Eng. 17 (2017) 207–215.
[19] G. Montes-Hernandez, et al., Removal of oxyanions from synthetic wastewater via carbonation process of calcium hydroxide: applied and fundamental aspects, J. Hazard. Mater. 166 (2009) 788–795.
[20] G. Montes-Hernandez, et al., Nanostructured calcite precipitated under hydrothermal conditions in the presence of organic and inorganic selenium, Chem. Geol. 290 (2011) 109–120.
[21] S. Hajji, et al., Arsenite and chromate sequestration onto ferrihydrite, siderite and goethite nanostructured minerals: isotherms from flow-through reactor experiments and XAS measurements, J. Hazard. Mater. 362 (2019) 358–367.
[22] G. Montes-Hernandez, N. Findling, F. Renard, Direct and indirect nucleation of magnetite nanoparticles from solution revealed by time-resolved raman spectroscopy, Cryst. Growth Des. 21 (2021) 3500–3510.
[23] G. Montes-Hernandez, F. Renard, Time-resolved in situ raman spectroscopy of the nucleation and growth of siderite, magnesite and calcite and their precursors, Cryst. Growth Des. 16 (2016) 7218–7230.
[24] G. Limousin, et al., Sorption isotherms: a review on physical bases, modeling and measurement, Appl. Geochem. 22 (2007) 249–275.
[25] G. Montes-Hernandez, F. Renard, Nucleation of brushite and hydroxyapatite from amorphous calcium phosphate phases revealed by dynamic in situ raman spectroscopy, J. Phys. Chem. C 124 (2020) 15302–15311.
[26] G. Montes-Hernandez, M. Bah, F. Renard, Mechanism of the formation of engineered magnesite: a useful mineral to mitigate CO2 industrial emissions, J. CO2 Util. 35 (2020) 272–276.
[27] G. Montes-Hernandez, et al., Amorphous calcium-magnesium carbonate (ACMC) accelerates dolomitization at room temperature under abiotic conditions, Cryst. Growth Des. 20 (2020) 1434–1441.
[28] T. Taut, R. Kleeberg, J. Bergmann, The new seifert rietveld program BGMN and its application to quantitative phase analysis, Mater. Sci. (Bulletin of the Czech and Slovak Crystallographic Association) 5 (1998) 55–64.
[29] G. Montes-Hernandez, et al., Sequential precipitation of a new goethite-calcite nanocomposite and its possible application in the removal of toxic ions from polluted water, Chem. Eng. J. 214 (2013) 139–148.
[30] F. Renard, et al., Selenium incorporation into calcite and its effect on crystal growth: an atomic force microscopy study, Chem. Geol. 340 (2013) 151–161.
[31] G. Montes-Hernandez, F. Renard, R. Lafay, Experimental assessment of CO2-mineral-toxic ion interactions in a simplified freshwater aquifer: implications for CO2 leakage from deep geological storage, Environ. Sci. Technol. 47 (2013) 6247–6253.
[32] F. Renard, et al., Interactions of arsenic with calcite surfaces revealed by in-situ nanoscale imaging, Geochim. Cosmochim. Acta 159 (2015) 61–79.
[33] A. Hamdouni, et al., Removal of Fe(II) from groundwater via aqueous portlandite carbonation and calcite-solution interactions, Chem. Eng. J. 283 (2016) 404–411.
[34] F. Renard, et al., Sequestration of antimony on calcite observed by time-resolved nanoscale imaging, Environ. Sci. Technol. 52 (2018) 107–113.
[35] M. Grønlie Guren, et al., Direct imaging of coupled dissolution-precipitation and growth processes on calcite exposed to chromium-rich fluids, Chem. Geol. 552 (2020), 119770.
[36] O. Giuffre, et al., Thermodynamic study on the interaction of ampicillin and amoxicillin with Ca2+ in aqueous solution at different ionic strengths and temperatures, J. Chem. Eng. Data 64 (2009) 800–809.
[37] G. Montes-Hernandez, et al., Formation of porous calcite mesocrystals from CO2-H2O-Ca(OH)2 slurry in the presence of common domestic drinks, CrystEngComm 17 (2005) 5725–5733.
[38] M.H. Zhang, Review on Fenton process for organic wastewater treatment based on optimization perspective, Sci. Total Environ. 670 (2019) 110–121.
[39] I. Gozlan, A. Rotstein, D. Avisar, Amoxicillin-degradation products formed under controlled environmental conditions: identification and determination in the aquatic environment, Chemosphere 91 (2013) 985–992.